Uzbekistan Journal of Polymers
journal homepage: https://uzpolymerjournal.com/
ISSN (online): 2181-3256 (print) 2181-3246

FORMATION AND CHARACTERIZATION OF POLYMER-DISSOLVING MICRONEEDLES FOR THE TRANSDERMAL DELIVERY SYSTEMS

*Khurshidabonu I. Burkhonova, *Khaydar E. Yunusov, *Abdushukur A. Sarymsakov, *Abdumutollib A. Atakhanov, **Guohua Jiang, ***Yanfang Sun

**Institute of Polymer Chemistry and Physics, Academy of Sciences of the Republic of Uzbekistan, Tashkent 100128, Uzbekistan.*
***School of Materials Science and Engineering, Zhejiang Sci-Tech University, Hangzhou 310018, China*
****College of Life Sciences and Medicine, Zhejiang Sci-Tech University, Hangzhou 310018, China*

ARTICLE INFO

Received: 12 February 2026
Revised: 16 February 2026
Accepted: 31 March 2025

Keywords:
Dissolving microneedles; polymer micromolding; hydroxypropyl methylcellulose; sodium-carboxymethylcellulose; polyvinyl alcohol; mechanical properties; plasticization; dissolution behavior; transdermal drug delivery systems.

Corresponding author
silver4727@yahoo.com

ABSTRACT

Dissolving polymer microneedles based on hydroxypropyl methylcellulose (HPMC), sodium carboxymethylcellulose (Na-CMC), polyvinyl alcohol (PVA), and their binary hydrogel blends were fabricated using a micromolding technique and systematically characterized. The influence of polymer type, concentration, viscosity, and blending on microneedle formation, mechanical properties, and dissolution behavior was investigated. Successful microneedle formation was achieved using 4–5% HPMC, 4–5% Na-CMC, and 10% PVA hydrogels, while all binary polymer systems (HPMC/CMC, HPMC/PVA, and CMC/PVA) demonstrated improved mold filling, tip sharpness, and structural stability.

FTIR analysis confirmed the presence of characteristic functional groups in HPMC, Na-CMC, and PVA and revealed pronounced intermolecular interactions in the polymer blends, primarily hydrogen bonding, dipole–dipole, and ion–dipole interactions, indicating enhanced molecular compatibility and structural integrity of the microneedle matrices. Mechanical testing showed that binary polymer systems exhibited improved mechanical properties compared with single-polymer microneedles. In particular, the HPMC/PVA blend demonstrated the highest tensile strength (98 MPa) and elongation at break (7%), indicating synergistic interactions between the polymers. The addition of glycerol as a plasticizer increased flexibility, with an optimal concentration of approximately 0.3 wt% providing a balanced combination of tensile strength and elongation.

Dissolution studies performed using an agarose-based skin model demonstrated rapid hydration and progressive dissolution of HPMC/CMC microneedles, with near-complete dissolution occurring within 10 min after insertion. These findings indicate that HPMC, Na-CMC, and PVA hydrogels, particularly their binary blends, represent promising polymer matrices for the development of dissolving microneedle systems for transdermal drug delivery applications.

DOI: *10.66640/UJP-2026-5-00003*

Introduction

Transdermal drug delivery systems (TDDS) using microneedle patch biomaterials are increasingly recognized as a promising alternative to traditional routes of biological active substance (BAS) administration [1]. They stand out for their non-invasiveness, patient comfort, ability to bypass first-pass metabolism, and potential for controlled release of BAS [2]. However,

the main limiting factor for the effectiveness of these systems is the outermost layer of the skin, which significantly hinders the penetration of many hydrophilic or high-molecular-weight drug molecules [3].

To overcome this barrier, microneedle (MN) technology has been developed, offering a minimally invasive approach to improve BAS delivery by creating microchannels through the skin layers without damaging its protective structure [4]. Microneedles are micron-sized projections that temporarily puncture the skin's surface without reaching deeper tissue layers, thereby facilitating efficient drug absorption while minimizing pain, inflammation, and the risk of infection [5]. Recently, microneedle platforms have gained attention for both drug delivery and bioanalytical applications, particularly microneedle-based biosensors for real-time physiological monitoring, demonstrating their versatile transdermal capabilities [6].

Among microneedle types, polymer dissolving microneedles (DMNs) are of particular interest [7]. These are fabricated from biodegradable and water-soluble polymers that completely dissolve upon insertion into the skin, delivering the drug directly into the dermal layers. They do not require removal and help minimize hazardous medical waste [8].

Polymeric microneedle systems can also be considered as a special class of polymeric drug forms, in which the polymer matrix performs not only a structural function but also regulates drug release kinetics, stability, and bioavailability. According to modern concepts of polymeric drugs, carrier polymers must be biodegradable, biocompatible, non-toxic, and capable of controlled degradation or dissolution in biological media [9]

The choice of polymer in DMN fabrication greatly affects their mechanical strength, mold release performance, and dissolution behavior, all of which play a critical role in defining their delivery mechanism [10]. Based on their behavior in the body, matrix polymers used for DMNs are typically classified into three groups [11]:

- water-soluble polymers such as hyaluronic acid, Na-CMC, HPMC, gelatin, chitosan derivatives, pectin, pullulan, and starch derivatives dissolve rapidly in the skin and release the drug immediately;
- swelling synthetic polymers such as PVA, polyethylene oxide (PEO), polyacrylic acid (PAA), poly(ethylene glycol) (PEG), and poly(N-vinyl alcohol-co-acrylamide) absorb interstitial fluid and release the drug gradually;
- biodegradable polymers such as poly(lactic-co-glycolic acid) (PLGA), polylactic acid (PLA), polycaprolactone (PCL), polyglycolic acid (PGA), poly(ortho esters), poly(anhydrides), poly(trimethylene carbonate), and polyhydroxyalkanoates (PHAs) do not dissolve in water but instead degrade enzymatically in the body into non-toxic products.

Polymers for ideal microneedle biomaterial fabrication should be biocompatible, non-toxic, mechanically stable, and capable of forming sharp, structurally intact needle tips. In this regard, cellulose derivatives such as HPMC and Na-CMC have been widely studied due to their water solubility, non-toxic, biodegrability, biocompatibility, film and microneedle forming ability [12]. However, in some cases -especially when using Na-CMC issues such as brittleness and insufficient tip formation have been observed [13].

Furthermore, PVA is a synthetic, water-soluble polymer known for its high mechanical strength, flexibility, and easy of processing [14]. It is widely used in biomedical applications such as wound dressings and drug delivery systems due to adhesive, non-toxic, skin-friendly, biocompatible, water soluble properties. When combined with polymers like HPMC, Na-CMC, PVA improves the structural integrity and mechanical properties of microneedles [15].

The mold casting method is considered one of the simplest, most cost-effective, and scalable techniques for fabricating microneedles. This method enables precise control over microneedle geometry and allows the drug to be incorporated directly into the polymer solution. However, the success of this technique depends heavily on the rheological properties of the polymer solution and the easy of mold demolding [16].

Microneedles of HPMC can form sharp tips with sufficient mechanical strength to penetrate the stratum corneum, while completely dissolving in aqueous environments without leaving residues on the skin [17].

Similarly, microneedles based on sodium-carboxymethylcellulose (Na-CMC) have attracted considerable attention due to their high hydrophilicity and rapid dissolution behavior. Although Na-CMC microneedles are capable of fast drug release upon insertion, their high brittleness and limited mechanical robustness often result in tip deformation or fracture during demoulding or skin insertion [18]. To overcome these limitations, Na-CMC is frequently blended with other polymers or plasticisers to improve its mechanical properties and structural integrity [19].

By contrast, PVA-based microneedles are renowned for their exceptional mechanical strength, flexibility and fracture resistance. PVA microneedles typically exhibit enhanced penetration capability and improved mould release performance compared to highly hydrophilic polymers. However, due to their swelling-dominated behaviour and relatively slow dissolution rate, PVA microneedles alone may not enable rapid drug release, unless they are combined with more water-soluble polymers [20]

Recent research has therefore focused increasingly on binary or hybrid polymer systems, in which HPMC or Na-CMC is blended with PVA in order to combine the rapid dissolution of the former with the enhanced mechanical stability of the latter. Composite microneedles made using this method have been reported to exhibit improved tip sharpness, a higher fracture force, controlled dissolution behaviour and more reliable drug release profiles than single-polymer systems [21].

Despite these advances, achieving an optimal balance between mechanical robustness, mold release efficiency and controlled dissolution remains challenging, particularly for hydrophilic, drug-loaded, dissolving microneedles. Therefore, a systematic investigation of HPMC, Na-CMC and PVA based microneedle matrices, as well as their binary combinations, is essential in order to develop microneedle systems that are mechanically stable, rapidly dissolve and are pharmaceutically viable.

In this study, dissolving microneedles were fabricated via mold casting using HPMC, Na-CMC, and PVA polymers - both individually and in combinations. The microneedles were evaluated for their morphology, structural integrity, and demolding behavior using optical microscopy. Na-CMC based microneedles were easily demolded, but exhibited brittleness and poor tip formation, with visible deformation during drying.

The aim of this study is to form dissolvable microneedles from individual and combined HPMC, Na-CMC, and PVA hydrogels, and to investigate their physicochemical properties.

Materials and Methods

2.1. Materials

For the fabrication of microneedles, the following polymer matrices were used: Industrial samples (“Promxim Impex” LLC, Uzbekistan) of purified Na-CMC ($C_6H_7O_2(OH)_{3-x}(OCH_2COONa)_x$, M.W. ~90.000–250.000) with a degree of substitution (DS) of 0.92 and a degree of polymerization (DP) of 1100 which obtained by method [22]. HPMC (2-Hydroxypropyl methyl cellulose ether, CAS No.: 9004-65-3, M.W. ~120.000) in contained 21.9% methoxy groups and 10.0% hydroxypropyl groups were purchased from Aladdin (China). Polyvinyl alcohol (PVA, $–[CH_2–CH(OH)]_n–$, CAS No.: 9002-89-5, M.W. ~85.000–124.000), glycerol ($C_3H_8O_3$, 99.5%, CAS No. 56-81-5) were purchased by Sigma-Aldrich (China) and used as an analytical grade polymer without further purification.

Agarose powder (analytical grade) was used to prepare a physical skin-mimicking hydrogel model for dissolution experiments. Agarose hydrogels were prepared at a concentration of 1.4 wt% (w/w) in phosphate-buffered saline (PBS, pH 7.4). To simulate the mechanical resistance of the stratum corneum during dissolution testing, a food-grade adhesive plastic film with a thickness of 14 ± 1 μm was used to cover the surface of the agarose hydrogel.

Polydimethylsiloxane (PDMS) microneedle molds with square pyramid-shaped cavities were purchased from Benteng Biotechnology Co., Ltd. (China). Pyramid-shaped microneedle formation molds with overall dimensions of 39 mm × 39 mm (array area: 29 mm × 29 mm), containing microneedles with a height of 800 μm, a base diameter of 330×330 μm, a tip diameter of 15 μm, and an inter-needle spacing of 260 μm, were used in this study. Distilled water was used as the primary solvent for the preparation of all polymer hydrogels. All chemicals and reagents used in this study were of analytical grade and were used as received unless otherwise stated.

2.2 Methods

2.2.1 Preparation of Na-CMC and HPMC hydrogel.

To prepare a 2%, 4%, and 5% solutions of Na-CMC and HPMC 2, 4 and 5 g. of purified Na-CMC and HPMC powders was gradually added to 98, 96 and 95 ml of distilled water and stirred at 60℃ temperature using a mechanical stirrer (OS20-S, India) at 1500 rpm/min for 2 hours until completely dissolved. To obtain a stable and homogeneous hydrogel, the mixture was treated with an ultrasonic disperser (UW-2200, Germany) operating at a sonication frequency of 44 kHz for 15 minutes. The resulting hydrogel was centrifuged via a centrifuge (CenLee 20K, China) at 10000 rpm for 15 minutes to remove undissolved particles and air bubbles.

2.2.2 Preparation of PVA hydrogels.

To prepare 5%, 8%, and 10% PVA hydrogels, 5, 8, and 10 g of PVA were gradually added to 95, 92, and 90 mL of distilled water, respectively, and stirred at 60 °C using a mechanical stirrer (OS20-S, India) at 1500 rpm for 2 hours until completely dissolved. To obtain a stable and homogeneous hydrogel, the mixture was treated with an ultrasonic disperser (UW-2200, Germany) operating at a vibration frequency of 44 kHz for 15 minutes. The resulting solution was then centrifuged using a centrifuge (CenLee 20K, China) at 10,000 rpm for 15 minutes to remove undissolved particles and air bubbles.

2.2.3 Preparation of HPMC/Na-CMC, Na-CMC/PVA and HPMC/PVA mixtures hydrogel.

To prepare the HPMC/Na-CMC, CMC/PVA, and HPMC/PVA hydrogel mixtures, the previously prepared individual hydrogels were combined at a 1:1 volume ratio. The mixtures were stirred at 60°C using a mechanical stirrer (OS20-S, India) at 1500 rpm for 2 hours until completely blended. To obtain a stable and homogeneous hydrogel, the mixtures were treated with an ultrasonic disperser (UW-2200, Germany) operating at a vibration frequency of 44 kHz for 15 minutes. The resulting hydrogels were then centrifuged using a centrifuge (CenLee 20K, China) at 10,000 rpm for 15 minutes to remove undissolved particles and air bubbles.

2.2.4 Fabrication of polymer-dissolving microneedles by the micromolding method.

Microneedles were fabricated using the micromolding method in molds with square pyramid-shaped cavities (10×10 mm), each needle being 800 μm in length. Polymer hydrogels were prepared by dissolving HPMC, Na-CMC, and PVA individually, as well as in combinations such as HPMC/Na-CMC, CMC/PVA, and HPMC/PVA, in distilled water. Glycerol was added as a plasticizer at concentrations ranging from 0.1 to 0.7 wt% relative to the total polymer mass in the hydrogel formulation. After glycerol addition, the mixtures were stirred at 60 °C until homogeneous solutions were obtained prior to microneedle casting. The prepared polymer hydrogels were carefully poured into the molds using a pipette. To ensure complete filling of the microneedle tips and to remove trapped air bubbles, the molds were placed in a vacuum chamber, and a pressure of 0.08–0.1 MPa was applied. As air bubbles migrated upward, the lower valve of the desiccator was slowly opened.

This vacuuming process was repeated 4 times. After vacuum treatment, the molds were left to dry at 35°C for 40–96 h. During the drying process, the molds were kept covered to prevent dust

contamination. After complete drying, the microneedle arrays were carefully demolded for further characterization. The method of microneedle fabrication is presented in Figure 1.

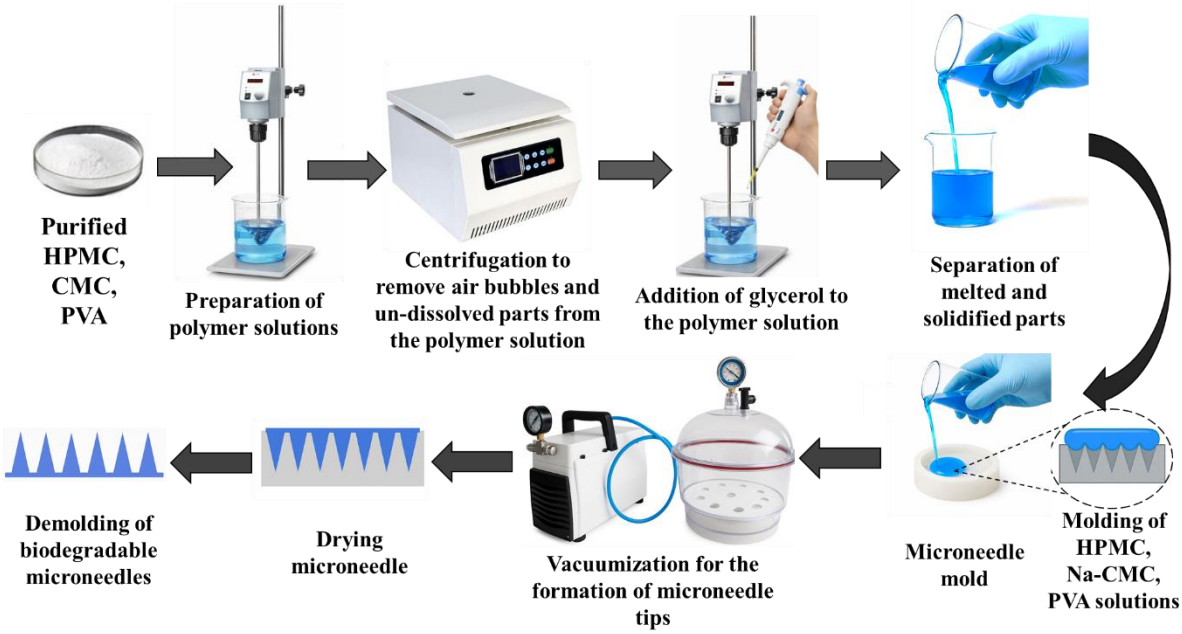

Figure 1. *Method for microneedle fabrication.*

2.2.5 Characterization of the polymer microneedles.

The chemical interactions and functional groups of Na-CMC, PVA, HPMC, and the polymer microneedle biomaterials were analyzed using a Fourier-transform infrared (FTIR) spectrometer (Inventio-S, Germany). FTIR spectra were recorded in the wavenumber range of 4000–500 cm^{-1} with a spectral resolution of 4 cm^{-1} and 32 scans were averaged for each sample to improve the signal-to-noise ratio.

The viscosity of HPMC (2%, 4%, 5%), Na-CMC (2%, 4%, 5%), and PVA (8%, 10%), as well as their 1:1 volumetric mixtures (HPMC/CMC (5%+5%); HPMC/PVA (5%+10%); CMC/PVA (5%+10%) hydrogel was determined by method of [23] using a rotational viscometer (IKA ROTAVISC lo-vi, Germany) at a controlled temperature of 20±0.1 °C. For each polymer solution, appropriate TSP-type spindles were selected based on the viscosity range. The spindle rotation speed was maintained within 20–60 rpm, while the instrumental load (rotational torque) was kept within the optimal range of 20–80%.

The mechanical properties of polymer microneedles were evaluated to assess their suitability for transdermal applications. Tensile strength and elongation at break were determined under uniaxial tension using a Zwick-1445 universal testing machine (Germany). The measurements were performed at ambient conditions, and the average values were calculated from at least three independent experiments.

2.2.6 Dissolution study of HPMC/CMC based microneedles using a physical skin model.

The dissolution behavior of HPMC/CMC based dissolving microneedles without biological active substance was investigated using a physical skin model in order to simulate biologically relevant conditions. An agarose hydrogel model was selected to avoid ethical concerns associated with animal experiments while adequately mimicking the dynamic viscoelastic properties of human skin [24].

Agarose hydrogels were prepared by dissolving agarose powder in phosphate-buffered saline (PBS, pH 7.4) at a concentration of 1.4 wt% (w/w) under heating with continuous stirring until a

clear solution was obtained. The hot agarose solution was then poured into Petri dishes and allowed to cool at room temperature to form uniform hydrogel slabs.

To simulate the mechanical resistance of the stratum corneum, the surface of the agarose hydrogel was covered with a food-grade adhesive plastic film with a thickness of 14±1 μm prior to microneedle insertion.

A total of five independent microneedle patches based on the HPMC/CMC polymer blend were prepared. Each microneedle patch had an initial mass of 0.154±0.006 g. The patches were individually inserted into the agarose hydrogel using a spring-loaded applicator to ensure consistent insertion conditions.

Each microneedle patch was removed from the skin model at a different predetermined time point: sample №1: 1 min, sample №2: 2 min, sample №3: 3 min, sample №4: 6 min, sample №5: 10 min.

After removal, each patch was gently dried at 35℃ temperature for 40-96 hours and weighed using an analytical balance. The dissolution of the polymer matrix was evaluated gravimetrically by calculating the percentage mass loss relative to the initial mass.

The percentage mass loss was calculated using Equation (1):

$$\text{Mass loss}_{\%}=\frac{m_0-m_t}{m_0}\times 100 \qquad (1)$$

Where, m_0-is the initial mass of the microneedle patch (0.154±0.006 g) and m_t-is the remaining mass at time t.

2.2.7 Microscopic investigation

The morphology and structural integrity of the fabricated microneedles were examined using an optical microscope. Microscopic observations were performed using a N-300M (UCMOS9000KPB) digital optical microscope (Ningbo Yongxin Optics Co., Ltd., China). The microneedle samples were observed at 2× and 4× magnifications to evaluate the uniformity of the microneedle array, tip sharpness, and surface morphology.

The obtained microscopic images were used to analyze the geometric parameters of the microneedles, including needle height, base width, and tip sharpness.

2.2.8 Statistical analysis

All quantitative data are presented as mean ± standard deviation (SD) based on at least three independent experiments.

Results and discussion

The primary fabrication techniques for microneedles include casting, hot pressing, injection molding, and mold casting, with the latter used in this study.

Hydrogels prepared from HPMC, Na-CMC, and PVA—both individually and in combinations such as HPMC/Na-CMC, Na-CMC/PVA, and HPMC/PVA—were uniformly spread onto the surface of the microneedle mold. The molds were then placed in a vacuum chamber, where a pressure of 0.08–0.1 MPa was applied to ensure complete filling of the cavities. Following centrifugation, the soluble microneedle arrays were dried and subsequently removed from the mold.

We observed that the required drying time depended on the polymer mass fraction in the formulation. Additionally, while drying temperature influenced the overall drying duration of composite microneedles, it had minimal impact on the molding quality. During the final stage of drying, the microneedles should be monitored at 10-minute intervals to determine the optimal endpoint.The drying temperature was set as 35℃ to facilitate timely observation of microneedle formation and timely removal of microneedles for the demolding operation. HPMC, Na-CMC, and PVA individually, as well as in combinations such as HPMC/CMC, CMC/PVA, and HPMC/PVA, were combined in different mass percentages to obtain the best microneedles with satisfactory

formability and high hardness that were not easy to fracture. The percentage of prepared soluble microneedles is shown in Table 1.

Polymer solutions were prepared both individually and in combination for microneedle fabrication (Table 1).

It can be seen from Table 1 that the ability of polymer solutions to form structurally stable microneedles depends strongly on the polymer type as well as its concentration and viscosity. As the polymer concentration increases, both the solution viscosity and the drying time required for microneedle formation also increase.

For HPMC solutions, microneedle formation was unsuccessful at a concentration of 2%, while increasing the concentration to 4% and 5% resulted in successful microneedle formation. This suggests that higher HPMC concentrations provide sufficient viscosity and mechanical strength necessary to maintain the microneedle geometry during the molding and drying processes (Table 1, №1-3).

Table 1

Formation of microneedles from different concentrations and ratio combinations of polymer solutions

№	Polymer samples	Concentration of polymer solution, %	Viscosity of solution (20°C), mPa·s	Drying time at 35°C, hour	Microneedle formability
1	HPMC	2	5600	40	–
2	HPMC	4	11885	60	+
3	HPMC	5	14387	72	+
4	Na-CMC	2	1433	40	–
5	Na-CMC	4	2823	60	+
6	Na-CMC	5	5264	72	+
7	PVA	5	1231	40	–
8	PVA	8	1664	60	–
9	PVA	10	2452	72	+
10	HPMC/CMC	5+5 (1:1)	8652	85	+
11	HPMC/PVA	5+10 (1:1)	10795	96	+
12	CMC/PVA	5+10 (1:1)	8325	85	+

Note: *(+) microneedle formation; (–) no formation microneedle.*

At 2% of Na-CMC concentration, no microneedle structures were obtained, whereas 4% and 5% Na-CMC solutions successfully formed microneedles. This indicates that, like HPMC, Na-CMC requires a certain minimum concentration to achieve the viscosity threshold needed for stable structure formation (Table 1, №4-6).

In contrast, PVA exhibited a different concentration-dependent behavior. Solutions containing 5% and 8% PVA were unable to form microneedles, while successful formation was only achieved at 10% PVA. This can be attributed to the relatively lower viscosity of PVA solutions at comparable concentrations, necessitating higher polymer content to obtain adequate mechanical rigidity (Table 1, №7-9).

Interestingly, all binary polymer combinations—HPMC/CMC (1:1, 5%+5%), HPMC/PVA (1:1, 5%+10%), and CMC/PVA (1:1, 5%+10%)—were able to produce well-formed microneedle structures. This observation highlights a synergistic effect between the polymers, where the combination of cellulose derivatives providing viscosity and film-forming ability with PVA contributing flexibility and mechanical strength leads to optimal structural integrity and moldability.

Overall, these results emphasize that solution viscosity is a critical determinant in microneedle fabrication. A minimum polymer concentration is required for each formulation to

ensure proper molding and drying behavior. Among the tested formulations, HPMC and Na-CMC at concentrations ≥4%, PVA at 10%, and their binary mixtures were identified as suitable candidates for producing robust and well-defined microneedle arrays.

The geometry, surface morphology, and tip sharpness of the polymer microneedles were examined using an optical microscope at 2× and 4× magnification, and the corresponding results are presented in Table 2.

It can be seen from Table 2, the microneedles obtained from all polymer hydrogels exhibited smooth needle surfaces.

The image shows a magnified view of microneedles obtained from a 4% of HPMC and Na-CMC hydrogels, displaying uniformly shaped, pyramid-like structures (Table 2, №1 and №3). The microneedles appear well-defined, with sharp tips and smooth lateral surfaces, indicating successful molding and polymer filling of the microneedle cavities.

Table 2

Results of microscopic investigation of microneedles obtained from different concentrations and ratio combinations of polymer solutions.

№	Polymer concentration and ratio	MN images Scale bar 400-500 µm	Microneedle formability characteristics
1	HPMC, 4%	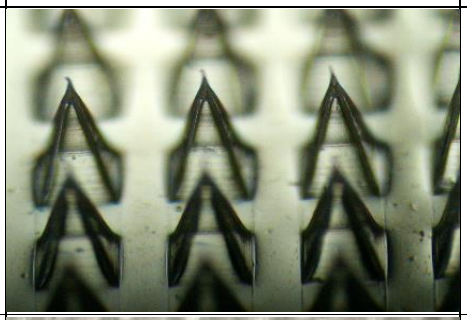	The needle tips are well-formed, low mechanical strength, many bubbles during drying, easily released from mold.
2	HPMC, 5%	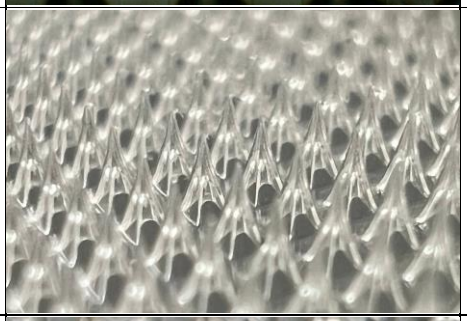	The needle tips are well-formed, low mechanical strength, many bubbles during drying, easily released from mold.
3	Na-CMC, 4%	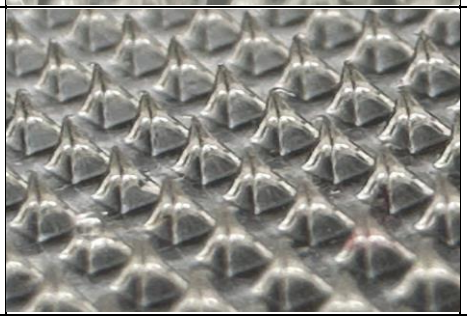	The needle tips are well-formed, brittle, thin, easily released from the mold with no air bubbles.

4	Na-CMC, 5%	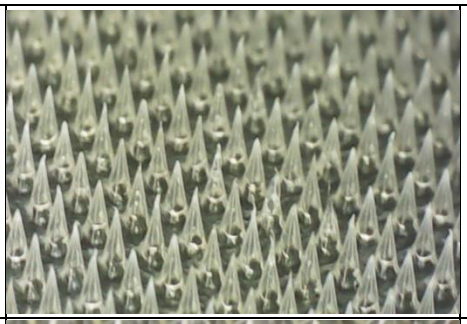	The needle tips are well-formed, hard, thick, easily released from the mold, no air bubbles, a little difficult to pour into the mold and there are air bubbles
5	PVA, 10%	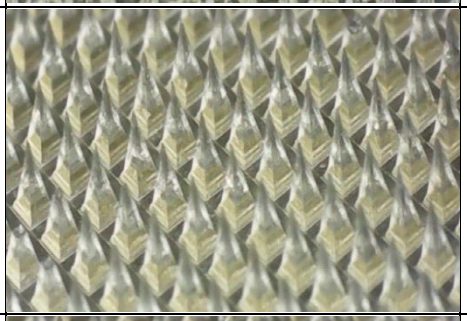	Strong, sharp-tipped, smooth and sufficiently capable of skin penetration, many bubbles during drying, well released from mold
6	HPMC/CMC, (1:1; 5%+5%)	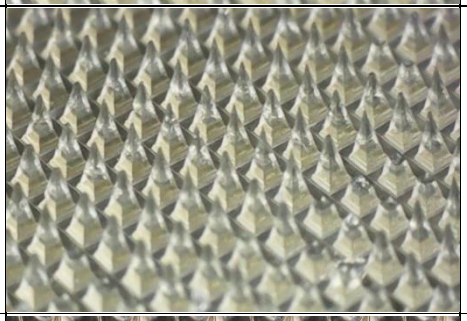	Needle tips are well shaped, slightly less durable, easily released from the mold, no bubbles.
7	HPMC/PVA, (1:1; 5%+10%)	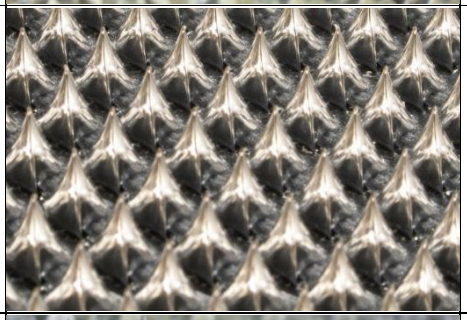	Needle tips are well-shaped, but the solution is not homogeneous and there are parts that remain unmixed, strong but there are air bubbles.
8	CMC/PVA, (1:1; 5%+10%)	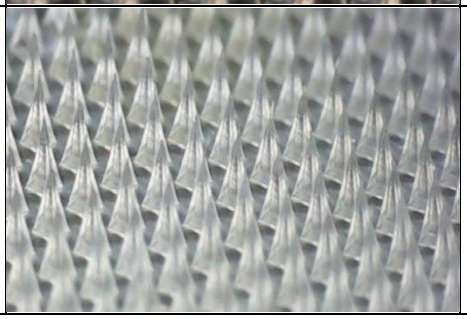	Needle tips well-formed, strong but brittle and fragile, easily released from the mold, no bubbles.

The high-magnification view of a microneedle array produced from 5% of HPMC and Na-CMC hydrogels. The microneedles display uniform geometry with well-defined, pyramid-like shapes and sharp tips (Table 2, №2 and №4). The array exhibits excellent structural regularity, indicating complete mold filling and successful replication of the microneedle features. The clarity and smoothness of the microneedle surfaces suggest good material homogeneity and proper drying conditions during fabrication.

The microneedle array fabricated from 10% PVA exhibits highly uniform, well-defined pyramid-like structures with smooth surfaces and sharp tips, indicating complete mold filling and good mechanical stability of the formulation (Table 2, №5). The clarity of the microneedle edges suggests effective drying and solidification, confirming that 10% PVA provides sufficient viscosity and structural integrity for high-quality microneedle formation.

The microneedles produced from the HPMC/CMC (1:1; 5%+5%), HPMC/PVA (1:1; 5%+10%), and CMC/PVA (1:1; 5%+10%) hydrogel combinations (Table 2, №6; №7; №8) exhibited well-formed, sharp needle tips with smooth surfaces, demonstrating adequate structural strength with slight brittleness, along with clean mold release and the absence of air bubbles.

To elucidate the interactions between functional groups in the HPMC/CMC, HPMC/PVA, and CMC/PVA systems, microneedles fabricated from their respective hydrogels were analyzed using FT-IR spectroscopy. The absorption profiles of the films were recorded in the range of 400–4000 cm^{-1}. The corresponding spectra are shown in Figure 2 (*curves* ***a–f***).

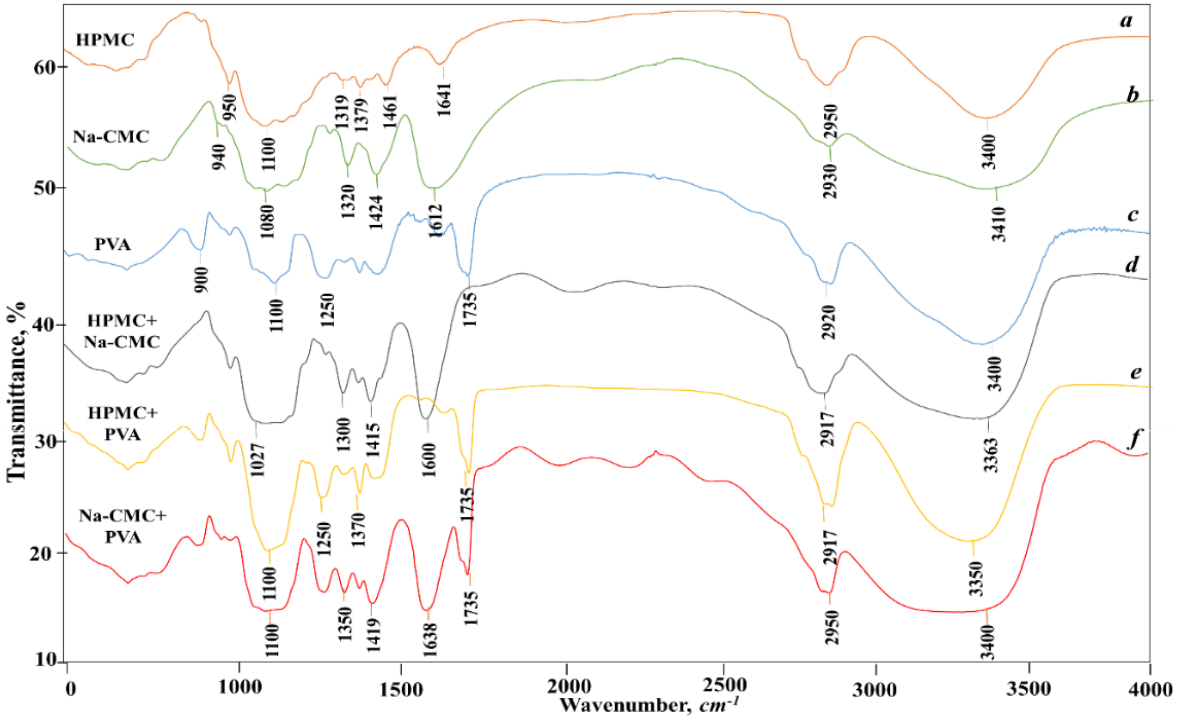

a. *HPMC;* ***b.*** *Na-CMC;* ***c.*** *PVA;* ***d.*** *HPMC/CMC,* ***e.*** *HPMC/PVA;* ***f.*** *CMC/PVA.*
Figure 2. *FTIR spectra of the microneedle samples obtained from polymer hydrogels.*

For HPMC, a broad absorption band at 3460 cm^{-1} is attributed to the stretching vibration of hydroxyl (−OH) groups involved in both intra- and intermolecular hydrogen bonding. The bands in the region of 2850–2950 cm^{-1} correspond to C–H stretching vibrations of the methyl and methylene groups, while the strong peaks at 1050–1150 cm^{-1} are assigned to C–O–C stretching vibrations of the ether linkages in the cellulose backbone (Fig. 2, *curve-**a***).

The spectrum of Na-CMC shows a characteristic asymmetric stretching of the carboxylate anion ($–COO^-$) at 1612 cm^{-1} and a symmetric stretching at 1424 cm^{-1}, confirming the presence of ionized carboxymethyl groups in the Na-CMC structure (Fig. 2, *curve-**b***).

The FTIR spectrum of PVA displays characteristic absorption band observed at 1735 cm^{-1} is attributed to the C=O stretching vibration of residual acetate groups, indicating the presence of partially hydrolyzed polyvinyl acetate segments in the PVA polymer chain. This confirms that the PVA sample is not fully hydrolyzed, as completely hydrolyzed PVA would lack this carbonyl

stretching band. Other typical absorption bands for PVA generally include a broad band around 3200–3500 cm^{-1}, corresponding to O–H stretching vibrations of hydroxyl groups involved in hydrogen bonding, and peaks near 2900 cm^{-1} associated with C–H stretching vibrations. The appearance of the 1735 cm^{-1} band therefore provides evidence of residual acetate functionality, influencing the polymer's hydrophilicity and film-forming behavior, which can affect the mechanical and dissolution properties of PVA-based microneedles (Fig. 2, *curve-**c***).

The FTIR spectrum of the HPMC/CMC microneedle formulation reveals notable spectral shifts indicative of intermolecular interactions between the two polymers. The broad –OH stretching band, which appears at 3460 cm^{-1} in the pure components, is shifted to 3363 cm^{-1} in the blended formulation. This pronounced shift toward a lower wavenumber suggests the formation of stronger hydrogen bonds between hydroxyl groups of HPMC and Na-CMC macromolecules, implying enhanced molecular compatibility and intermolecular association within the polymer matrix. Furthermore, the C–O–C stretching vibrations observed in the region of 1050–1100 cm^{-1} become broader and less intense in the blend compared to the individual polymers. This broadening and reduction in intensity further confirm molecular-level interactions and possible rearrangement of the polymeric network due to hydrogen bonding. Such interactions contribute to improved mechanical strength, uniformity, and stability of the microneedle structure, which are essential for effective microneedle fabrication and performance (Fig. 2, *curve-**d***).

The FTIR spectra of the polymer blends provide clear evidence of intermolecular interactions between the constituent polymers. In the HPMC/PVA blend, the characteristic carbonyl absorption band of PVA remains visible, confirming the presence of residual acetate groups. Meanwhile, the broad –OH stretching vibration shifts from 3440 to 3365 cm^{-1}, indicating the formation of hydrogen bonds between the hydroxyl groups of HPMC and the carbonyl groups of PVA. This spectral shift toward a lower wavenumber reflects stronger hydrogen bonding and enhanced compatibility between the two polymer matrices, which likely contributes to improved mechanical integrity and homogeneity of the microneedle structure (Fig. 2, *curve-**e***).

In the CMC/PVA composite, the FTIR spectrum exhibits both the C=O stretching band at 1735 cm^{-1} corresponded to PVA and the COO^- asymmetric and symmetric stretching bands at 1638 and 1419 cm^{-1}, respectively, corresponding to Na-CMC. The simultaneous presence of these bands suggests the occurrence of ion–dipole interactions between the negatively charged carboxylate groups of Na-CMC and the hydroxyl or carbonyl groups of PVA. Additionally, the broad absorption around 3400 cm^{-1} indicates the existence of extensive hydrogen bonding within the polymer matrix. These combined interactions result in enhanced miscibility and structural stability of the CMC/PVA blend, which are beneficial for maintaining the desired morphology and mechanical strength of the microneedles (Fig. 2, *curve-**f***).

Overall, the FTIR analysis confirms that blending HPMC, Na-CMC, and PVA results in pronounced intermolecular interactions, primarily through hydrogen bonding, dipole–dipole, and ion–dipole interactions. These intermolecular interactions are consistent with the mechanical testing results presented in Table 3. In particular, the HPMC/PVA blend exhibited the highest tensile strength (98 MPa), indicating enhanced mechanical stability resulting from synergistic interactions between HPMC and PVA.

The presence of ionogenic carboxylate groups in Na-CMC plays a crucial role in intermolecular interactions and structural stabilization of polymer matrices. Such functional groups are known to participate in coordination and electrostatic interactions, contributing to enhanced composite stability [25].

The mechanical properties of microneedle biomaterials play a crucial role in their practical application [26].

For polymer-based microneedles, moderate to high tensile strength is desirable to prevent cracking during handling, demolding, and insertion. Materials with very low tensile strength may fail even before application, while excessively rigid materials may become brittle. Thus,

microneedle biomaterials should exhibit sufficient tensile strength to maintain structural integrity, particularly at the needle base and tip, where stress concentration is highest. [27]

While high strength is essential, microneedles must also possess a degree of elasticity. A moderate level of ductility allows microneedles to absorb mechanical stress during insertion and minor lateral movements without cracking. Therefore, biomaterials should demonstrate limited but sufficient elongation, providing toughness without excessive flexibility that could cause bending instead of penetration [28].

Therefore, the tensile strength and elongation at break of microneedles prepared from Na-CMC, PVA, and HPMC polymer solutions were investigated. The obtained results are summarized in Table 3.

As shown in Table 3, microneedles fabricated from polymer solutions with increasing concentration exhibited enhanced tensile strength, while the elongation at break increased from approximately 4% to 5%. HPMC microneedles showed an increase in tensile strength from 86 MPa (4%) to 93 MPa (5%), along with a slight rise in elongation at break from 3% to 4% (Table 3, №1 and №2). A similar trend was observed for Na-CMC, where tensile strength increased from 70 MPa to 78 MPa, and elongation rose from 4% to 5% as concentration increased from 4% to 5% (Table 3, №3 and №4).

Table 3

Tensile strength at break and elongation at break of polymer microneedle biomaterials

№	Microneedle material type	Polymer hydrogel concentration, %	Tensile strength at break, MPa	Elongation at break, %
1	HPMC	4	86±2	3±0.5
2	HPMC	5	93±2	4±0.5
3	Na-CMC	4	70±2	4±0.5
4	Na-CMC	5	78±2	5±0.5
5	PVA	10	54±2	6±0.5
6	HPMC/CMC	5+5 (1:1)	86±2	5±0.5
7	HPMC/PVA	5+10 (1:1)	98±2	7±0.5
8	CMC/PVA	5+10 (1:1)	85±2	4±0.5

In contrast, PVA (10%) exhibited the lowest tensile strength (54 MPa) but the highest elongation at break (6%), indicating greater flexibility and ductility. While PVA contributes elasticity, its lower strength may limit its suitability as a sole structural material for microneedles that must withstand insertion forces (Table 3, №5).

The HPMC/CMC (1:1) blend maintained a tensile strength (86 MPa) comparable to 4% HPMC but increased elongation to 5%, suggesting that CMC contributed to improved ductility without severely compromising strength (Table 3, №6).

More pronounced synergistic effects were observed in blends containing PVA. The HPMC/PVA (1:1) formulation showed the highest tensile strength (98 MPa) and highest elongation (7%) among all tested samples (Table 3, №7). This indicates a complementary interaction where HPMC provides structural rigidity and PVA enhances flexibility, resulting in a tougher and more fracture-resistant material.

In contrast, the CMC/PVA (1:1) blend achieved moderate tensile strength (85 MPa) and limited elongation (4%), suggesting that the reinforcing effect of CMC is weaker than that of HPMC when combined with PVA (Table 3, №8). This highlights the importance of polymer compatibility and intermolecular interactions in determining the final mechanical performance.

The mechanical properties of microneedles are strongly influenced by polymer type, concentration, and blending. Increasing polymer concentration improved both tensile strength and elongation for HPMC and Na-CMC systems. Among single polymers, HPMC provided higher

strength, while PVA contributed greater flexibility but insufficient mechanical robustness on its own.

These results are in agreement with the FTIR analysis, which revealed strong intermolecular interactions within the polymer blends. In particular, the superior mechanical performance of the HPMC/PVA system may be attributed to synergistic interactions between HPMC and PVA, resulting in improved mechanical stability of the microneedle matrix.

To reduce the brittleness and fracture tendency of the microneedle biomaterials, plasticization studies were conducted. Medical-grade glycerol, approved for biomedical applications, was selected as a plasticizer. Various concentrations of glycerol were added to the initial polymer solutions to improve elongation at break. The effect of glycerol content on the tensile strength and elongation of microneedles is presented in Table 4.

It can be seen from the results in Table 4 that the incorporation of glycerol leads to a decrease in tensile strength accompanied by a significant increase in elongation at break. This behavior can be explained by the penetration of the plasticizer into the intermolecular spaces of polymer macromolecules, which reduces chain orientation and intermolecular interactions.

For single 5% of HPMC hydrogel based microneedle exhibited the highest tensile strength of 93 MPa in the absence of glycerol, but its strength decreased sharply to 25 MPa at 0.7 wt% glycerol. A similar trend was observed for 5% of Na-CMC and of 10% PVA, where tensile strength declined with increasing glycerol content, while elongation at break increased, indicating enhanced flexibility. Among these, Na-CMC maintained relatively balanced mechanical properties at moderate glycerol levels (0.3 wt%), preserving sufficient strength while improving ductility (Table 4, №1-3).

Table 4

Effect of glycerol plasticizer content on tensile strength and elongation at break of polymer microneedle biomaterials

№	Microneedle material type	Glycerol content, wt%	Tensile strength at break, MPa	Elongation at break, %
1	HPMC (5%)	-	93	4
		0.1	68	5
		0.2	52	7
		0.3	**47**	**8**
		0.5	33	8
		0.7	25	9
2	Na-CMC (5%)	-	78	5
		0.1	62	7
		0.2	57	8
		0.3	**45**	**9**
		0.5	34	10
		0.7	28	10
3	PVA (10%)	-	54	6
		0.1	48	8
		0.2	42	9
		0.3	**39**	**9**
		0.5	29	10
		0.7	23	11
4	HPMC/CMC; 5+5 (1:1)	-	86	5
		0.1	78	8
		0.2	64	8
		0.3	**48**	**9**
		0.5	32	10

		0.7	22	10
5	HPMC/PVA; 5+10 (1:1)	- 0.1 0.2 **0.3** 0.5 0.7	98 85 74 **48** 31 25	7 8 8 **9** 10 11

Blended systems, including HPMC/CMC (5+5, 1:1) and HPMC/PVA (5+10, 1:1), initially showed higher tensile strength compared to most single-polymer matrices, suggesting synergistic interactions between the components. Among the investigated polymer systems, the HPMC/PVA blend exhibited the highest tensile strength (98 MPa) in the absence of glycerol, indicating enhanced mechanical stability due to synergistic interactions between HPMC and PVA. However, these blends also showed a marked reduction in tensile strength with glycerol addition beyond 0.3 wt%, while elongation at break increased steadily, reaching up to 11–10% at 0.7 wt% glycerol (Table 4, № 4-5).

Overall, the data indicate that low to moderate glycerol content at 0.3 wt% provides an optimal balance between tensile strength and elongation. At these levels, microneedle biomaterials retain sufficient structural integrity to withstand handling and insertion, while acquiring adequate flexibility to resist brittle fracture.

Glycerol effectively acts as a plasticizer for polymer-based microneedle materials, enhancing flexibility but decreasing tensile strength. Careful optimization of glycerol content is essential to achieve a balance between mechanical robustness and ductility, ensuring safe and efficient transdermal delivery applications.

The dissolution behavior of HPMC/CMC-based dissolving microneedles under skin-mimicking conditions is illustrated in Figure 3. The results clearly demonstrate a time-dependent and progressive dissolution of the microneedle polymer matrix.

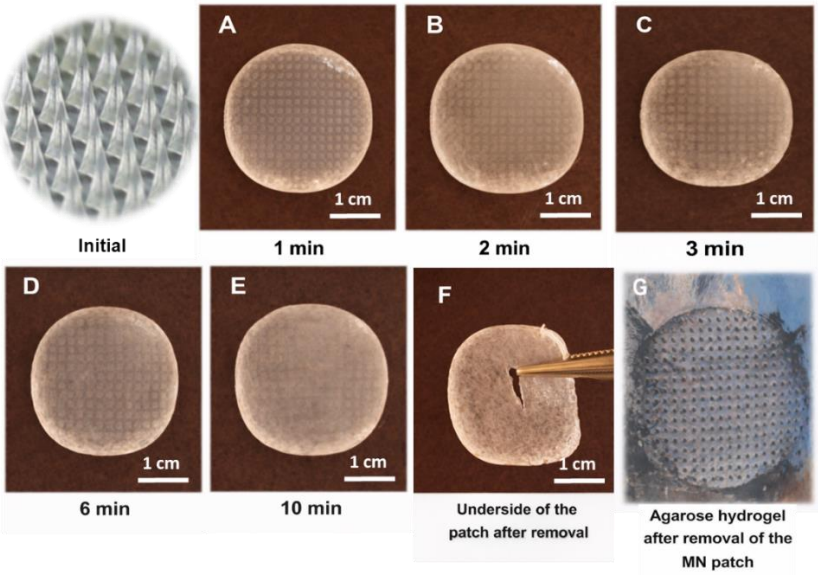

*Initial microneedle morphology prior to insertion and optical images of microneedle patches after 1, 2, 3, 6, and 10 min of insertion into the agarose hydrogel **(A–E)**. Underside of the patch after removal **(F)**. Agarose hydrogel surface showing puncture marks after microneedle removal **(G)**.*

Figure 3. Dissolution behavior of HPMC/CMC microneedles in an agarose-based skin model. *Scale bar: 1 cm.*

The initial microneedle structure, prior to insertion into the skin model, is shown in Figure 3A, where the microneedles exhibit a well-defined geometry and sharp tips, confirming their structural integrity before dissolution.

After 1 min of contact with the agarose hydrogel, partial hydration and the onset of matrix dissolution were observed (Figure 3B). Although the microneedle tips remained visible, gravimetric analysis revealed a mass reduction of approximately 18–22%, indicating rapid water uptake by the hydrophilic HPMC/CMC matrix.

At 2 and 3 min, the dissolution process accelerated significantly. As shown in Figure 3C, the microneedle structures lost their geometric definition, corresponding to a mass loss of approximately 35–55%. This stage reflects the progressive disintegration of the polymeric microneedle matrix.

After 6 min, extensive dissolution of the microneedles was evident (Figure 3D and 3E), with the majority of the polymer matrix dissolved and a mass loss of approximately 65–70%. At this point, the microneedle structures were largely disintegrated.

Following 10 min of insertion, the dissolvable portion of the microneedle patch was almost completely dissolved, leaving only the backing layer intact, as shown in Figure 3F. The remaining mass was below 5% of the initial mass, indicating near-complete dissolution of the HPMC/CMC microneedle matrix.

The puncture marks observed on the agarose hydrogel surface after removal of the microneedle patches (Figure 3G) confirm successful penetration of the microneedles into the skin model and demonstrate that dissolution occurred after insertion rather than prior to penetration.

Overall, the visual observations and gravimetric measurements consistently indicate that HPMC/CMC microneedles undergo rapid hydration and complete dissolution within a short period under skin-mimicking conditions. This dissolution behavior provides a strong structural basis for the subsequent incorporation of active pharmaceutical ingredients and supports the suitability of the HPMC/CMC polymer system for dissolving microneedle-based transdermal drug delivery applications.

Conclusion

In this study, dissolving polymer microneedles were successfully fabricated using HPMC, Na-CMC, and PVA polymers, both individually and in binary combinations, through a micromolding technique. The results demonstrated that polymer concentration, viscosity, and intermolecular interactions play a critical role in determining microneedle formation, structural integrity, and mechanical performance.

Single-polymer microneedles prepared from HPMC (4–5%), Na-CMC (4–5%), and PVA (10%) were capable of forming microneedle arrays; however, each system exhibited certain limitations, such as brittleness in Na-CMC or relatively lower mechanical strength in PVA. In contrast, binary polymer systems showed improved structural and mechanical properties due to synergistic interactions between the polymer components.

FTIR analysis confirmed the presence of strong intermolecular interactions, including hydrogen bonding and ion–dipole interactions, within the blended polymer matrices. These interactions contributed to enhanced molecular compatibility and improved mechanical stability of the microneedle structures. Mechanical testing further demonstrated that the HPMC/PVA blend exhibited the highest tensile strength (98 MPa) and elongation at break (7%), indicating an optimal balance between rigidity and flexibility.

The incorporation of glycerol as a plasticizer significantly improved the flexibility of microneedle materials, while moderate glycerol content (approximately 0.3 wt%) provided an optimal balance between tensile strength and elongation. Dissolution studies performed using an agarose-based skin-mimicking model confirmed that HPMC/CMC microneedles undergo rapid

hydration and near-complete dissolution within 10 min after insertion, while maintaining sufficient mechanical stability for penetration.

Overall, the obtained results demonstrate that HPMC/CMC, HPMC/PVA, and CMC/PVA polymer blends represent promising matrices for the fabrication of mechanically stable and rapidly dissolving microneedles. These systems provide a solid foundation for future studies involving drug loading, controlled release, and in vivo evaluation for transdermal drug delivery applications.

Acknowledgment: *This work was supported by the fundamental program of Academy of Sciences of the Republic of Uzbekistan "Scientific foundations of the functionalization of natural biopolymers and their derivatives for the purpose of activation" for the year 2026.*

CRediT authorship contribution statement: Burkhonova Khurshidabonu I.: *Investigation, Writing-Original Draft & Methodology;* ***Yunusov Khaydar E:*** *Writing-Original Draft, Investigation Methodology,* ***Sarymsakov Abdushkur A:*** *Interpretations & Conceptualization;* ***Atakhanov Abdumutolib A:*** *Editing, Conceptualization;* ***Guohua Jiang:*** *Writing, Editing & Interpretations;* ***Yanfang Sun:*** *Supervision & Interpretations.*

Declaration of interests: *The authors declare that they have no known competing financial interests or personal relationships that could have appeared to influence the work reported in this paper.*

Data availability statement: *The data that support the findings of this study are available on request from the corresponding author. The data are not publicly available due to privacy or ethical restrictions.*

REFERENCES

[1]. Crasta A., Painginkar T., Sreedevi A., Pawar S.D., Sathyanarayana M.B., Vasantharaju S.G., Osmani R.A.M., Ravi G.. Transdermal drug delivery system: A comprehensive review of innovative strategies, applications, and regulatory perspectives. OpenNano, 2025, V.24, pp.100245. https://doi.org/10.1016/j.onano.2025.100245.

[2]. Shah S.W.A., Li X., Yuan H., Shen H., Quan S., Pan G., Ishfaq M., Shah A. U., Xie H., Shao J. Innovative transdermal drug delivery systems: Benefits, challenges, and emerging application. BMEMat. 2025, e70001. https://doi.org/10.1002/bmm2.70001.

[3]. Prausnitz M. R., Langer R. Transdermal drug delivery. Nature Biotechnology, 2008, V.26, I.11, pp.1261–1268. https://doi.org/10.1038/nbt.1504.

[4]. Prausnitz M. R., Mitragotri S., Langer R. Current status and future potential of transdermal drug delivery. Nature Reviews Drug Discovery, 2004. V.3, I.2, pp.115–124. https://doi.org/10.1038/nrd1304.

[5]. Shivaswamy H.R., Binulal P., Benoy A., Lakshmiramanan K., Bhaskar N., Pandya H. J. Microneedles as a Promising Technology for Disease Monitoring and Drug Delivery: A Review. ACS Mater. Au 2025, V.5, I.1, pp.115–140. https://doi.org/10.1021/acsmaterialsau.4c00125.

[6]. Yao R., Wu Z., Olatunji O.Y., Yunusov Kh.E., Turakulov F.M., Chen J., Jiang G. In-situ blood glucose level detection based on a non-enzymatic microneedle biosensor. Microchemical Journal, 2025. V.219, pp. 115991. https://doi.org/10.1016/j.microc.2025.115991

[7]. Larrañeta E., McCrudden M.T.C., Courtenay A.J., Donnelly R.F. Microneedles: A new frontier in nanomedicine delivery. Pharmaceutics, 2016. V.8, I.2, pp.22. https://doi.org/10.1007/s11095-016-1885-5.

[8]. Moawad F., Pouliot R., Brambilla D. Dissolving microneedles in transdermal drug delivery: A critical analysis of limitations and translation challenges. Journal of Controlled Release. 2025, V.383, pp.113794. https://doi.org/10.1016/j.jconrel.2025.113794.

[9]. Sarymsakov A.A., Yunusov Kh.E. Perspectives on creating polymeric drugs. Uzbekistan Journal of Polymers, 2022. V.1, I.1, pp. 61–68. http://uzpolymerjournal.com/articles/article.php?id=220106.

[10]. Shaik S., Prusty S., Choudhury A., Biswal T., Biswal B. Comparison of polymers to enhance mechanical properties of microneedles for bio-medical applications. Micro and Nanosystems Letters. 2020, V.8, I.1, pp.1–9. https://doi.org/10.1186/s40486-020-00113-0.

[11]. Wang R., Jiang G., Aharodnikau E.U., Yunusov Kh.E., Sun Y., Liu T., Solomevich O.S. Recent Advances in Polymer Microneedles for Drug Transdermal Delivery: Design Strategies and Applications. Macromol. Rapid Commun. 2022, V.43, I.8, e2200037. https://doi.org/10.1002/marc.202200037.
[12]. Ita K. Dissolving microneedles for transdermal drug delivery. Advances and challenges: Biomedicine & Pharmacotherapy. 2017, V.93, pp.1116–1127. https://doi.org/10.1016/j.biopha.2017.07.019.
[13]. Zhou Q., Li Z., Jiang H., Chen X., Zhang Z., Huang Y. Preparation and properties of polyvinylpyrrolidone/sodium carboxymethyl cellulose composite soluble microneedles. Pharmaceuticals. 2023, V.16, I.5, pp.759. https://doi.org/10.3390/ph16050759.
[14]. Liang Y., Zhao Y., Gao X., Zhang S., Qiu Y., Li Q. Mechanical strength affecting the penetration in microneedles and their applications. Biomedicine & Pharmacotherapy. 2024, V.174, pp.114034. https://doi.org/10.1016/j.biopha.2024.114034.
[15]. Mao Y., Zhang X., Rui Y., Zhong Ch., Yunusov Kh.E., Zhong Sh., Pan J., Jiang G. Fabrication of hollow microneedles with double-layer shell structure for rapid and prolonged local anesthesia. J Drug Delivery Science and Tech, 2025. V.104, e106516. https://doi.org/10.1016/j.jddst.2024.106516.
[16]. Zhang Y., Ma G. Polymer materials and solvent casting micromolding method for fabrication of dissolving microneedles. Journal of Controlled Release, 2022. V.344, pp.492–512. https://doi.org/10.1016/j.jconrel.2021.12.022.
[17]. Wang R., Sun Y., Wang H., Liu T., Shavandi A., Nie L., Yunusov Kh.E., Jiang G. Core–shell structured microneedles with programmed drug release functions for prolonged hyperuricemia management. J Materials Chemistry B, 2024. V.12, I.4, pp1064-1076. https://doi.org/10.1039/D3TB02607H
[18]. Jana B.A., Osmani R.A., Jaiswal S. Fabrication of Carboxymethylcellulose-Gelatin Dissolving Microneedle Patch for Pain-Free, Efficient, and Controlled Transdermal Delivery of Insulin. J Pharm Innov, 2023. V.18, pp.653–664. https://doi.org/10.1007/s12247-022-09670-w.
[19]. Liu T., Sun Y., Jiang G., Zhang W., Wang R., Nie L., Shavandi A., Yunusov Kh.E., Aharodnikau U.E., Solomevich S.O. Porcupine-inspired microneedles coupled with an adhesive back patching as dressing for accelerating diabetic wound healing. Acta Biomaterialia, 2023. V.160, pp32–44. https://doi.org/10.1016/j.actbio.2023.01.059.
[20]. Ando D., Miyatsuji M., Sakoda H., Yamamoto E., Miyazaki T., Koide T., Sato Y., Izutsu K.I. Mechanical Characterization of Dissolving Microneedles: Factors Affecting Physical Strength of Needles. Pharmaceutics, 2024. V.16, pp.200. https://doi.org/10.3390/pharmaceutics16020200.
[21]. Wang R., Wang H., Yao R., Li Y., Manar S., Nie L., Yunusov K.E., Pan J., Jiang G. Iontophoresis-driven transdermal drug delivery system based on porous microneedles for hyperuricemia treatment. International Journal of Pharmaceutics, 2025. V.671, pp125290. https://doi.org/10.1016/j.ijpharm.2025.125290.
[22]. Yuldoshov Sh.A., Yunusov Kh.E., Sarymsakov A.A., Goyibnazarov I.Sh. Synthesis and characterization of sodium carboxymethylcellulose from cotton, powder, microcrystalline and nanocellulose. Polymer Engineering and Science. 2022, V.62, pp.677–686. https://doi.org/10.1002/pen.25874.
[23]. Chakraborty B.C., Ratna D. Elastic deformation-Hookean solid. Polymers for Vibration Damping Applications. 2020, pp.143-201, https://doi.org/10.1016/B978-0-12-819252-8.00004-5.
[24]. Silva A.C.Q., Pereira B., Lameirinhas N.S., Costa P.C., Almeida I.F., Dias-Pereira P., Correia-Sá I., Oliveira H., Silvestre A.J.D., Vilela C., Freire C.S.R. Dissolvable carboxymethylcellulose microneedles for noninvasive and rapid administration of diclofenac sodium. Macromolecular Bioscience. 2022, V.22, e2200323. https://doi.org/10.1002/mabi.202200323.
[25]. Yunusov Kh.E., Sarymsakov A.A. Recent advances in the creation of polymer forms drugs with silver nanoparticles for medical purposes. Uzbekistan Journal of Polymers, 2022. V.1, I.2, pp15–24. http://uzpolymerjournal.com/articles/article.php?id=220202.
[26]. Tsuboko Y, Sakoda H, Okamoto Y, Nomura Y, Yamamoto E. Mechanical Characterization of Individual Needles in Microneedle Arrays: Factors Affecting Compression Test Results. Pharmaceutics. 2024; V.16, I.11, pp.1480. https://doi.org/10.3390/pharmaceutics16111480.
[27]. Zhang Z, Du G, Sun X, Zhang Z. Viscoelastic Properties of Polymeric Microneedles Determined by Micromanipulation Measurements and Mathematical Modelling. Materials. 2023; V.16, I.5, pp.1769. https://doi.org/10.3390/ma16051769.
[28]. Makvandi P., Kirkby M., Hutton A.R.J., Shabani M, Yiu C.K.Y., Baghbantaraghdari Z., Jamaledin R., Carlotti M., Mazzolai B., Mattoli V., Donnelly R.F. Engineering Microneedle Patches for Improved Penetration: Analysis, Skin Models and Factors Affecting Needle Insertion. Nanomicro Lett. 2021, V.16, I.13, pp.93. https://doi.org/